The available power obtainable from tidal stream turbines from a flow around an idealised headland

Thomas A.A. Adcock(1)

(1) *Department of Engineering Science, University of Oxford. thomas.adcock@eng.ox.ac.uk*

Abstract

Many candidate sites for tidal stream energy extraction can be classified as headland sites. Understanding the tidal resource of such sites is of fundamental importance to the industry. This paper examines an upper bound for the power might be generated from an idealised headland. The dependence of this on length of turbine rows, number of turbine rows and turbine blockage ratio are examined. Conclusions are drawn from this which are applicable to real headland sites.

Keywords: Tidal stream turbine; resource assessment; headland

1. Introduction

Many candidate sites for tidal energy extraction may be classified as headland sites. Examples include Anglesey, Portland Bill, and the Isle of Wight. To develop tidal turbine farms at these sites it is important to be able to understand the characteristics of the tidal energy resource. Currently many different devices are under development and the amount of energy a particular site can produce will be dependent on the actual type of turbine used. In this paper we do not seek to examine the power a particular device will generate but instead examine the upper bound for the power which can be produced. An upper bound which has traditionally been used is the extractable energy of the site. However, a lower bound than this can be obtained by examining the power available for generation using actuator disc models to represent the inviscid limit on the power which can be generated by rows of tidal turbines. As more turbines are added the power per swept area of turbine falls until this drops below some cut off beyond which any extra power generation is unfeasible. For this paper considering an idealised problem, we just examine the general trends of how the power per swept area varies with turbine length and number of rows.

This paper analyses an idealised tidal headland using a depth-integrated numerical model. The objective of this work is to understand the general characteristics of a headland sites. Whilst all real locations will have slightly different characteristics the aim of this paper is to establish some general, qualitative, trends which will be useful in analysing real locations. In particular we look at how the available power varies with number of turbine rows, length of turbine rows and the blockage ratio of the turbines (the fraction of the water column they take up).

Draper et al. (2013a) analysed a similar idealised headland (although with a different geometry to the one in this study). Their study looked in detail at how tidal turbines modified the flow field around the headland and at the energy extraction. A number of other studies of headland sites have been made (e.g. Blunden & Bahaj (2006); Draper et al. (2013b); Serhadlıoğlu (2013a); Adcock & Draper (2014a)) but none of these have looked at the aspects explored in this paper.

2. Numerical model

2.1 Numerical scheme

The numerical model used in this paper is the discontinuous Galerkin (DG) version of ADCIRC (Kubatko et al., 2006, 2009). The model solves the shallow water equations which are typically used for tidal modelling. The numerical scheme has been verified and validated for various applications such as modelling tidal flows and storm surges.

In this study we are modelling a headland site. The shallow water equations used here are known to give an imperfect model for the flow around a headland (Stansby, 2006). Nevertheless, the purpose of this study is to establish the leading order effects of placing rows of turbines off headlands and we are confident that our model simulates the physics of a real site sufficiently well to achieve this.

2.2 Inclusion of tidal devices

We represent tidal turbines in the model as a line discontinuity following the approach of (Draper et al., 2010). This method imposes a change in the water level across the lines of turbines in the model. The change in water depth across the turbines is given by the finite Froude number actuator disc theory (Houlsby et al., 2008). The turbine characteristics are thus a function of upstream Froude number, Fr (non-dimensionalised flow speed), blockage ratio, B (the proportion of the water column swept by turbines), and wake velocity coefficient, α_4 (the velocity, relative to upstream of the flow which has passed through the turbines, at a distance downstream where local pressures have equalised). This model for the turbines gives both the "extracted power" and "available power". The extracted power is the power removed from the flow and is not considered in this paper. The available power is the extracted power minus the power lost in the inevitable mixing behind the turbines and thus constitutes an upper limit on the power which could be generated. Real turbines will, of course, not operate as efficiently as this and there will be additional losses due to the turbine support structure which are not considered in this paper.

The numerical implementation and verification of this into the DG ADCIRC code is described in Serhadlıoğlu (2013b). In this implementation, the turbine properties (α_4 and B) are assigned to nodes. The edges where turbines are placed (and hence the Gaussian points within these elements) will take the average value of the turbine properties assigned to the nodes which define the edge. The tidal turbines' blockage is based on the blockage at mean sea level – i.e. the area of the turbine remains the same causing a small change in blockage over the tidal cycle as the water level rises and falls. The model has been used to analyse tidal energy extraction from ocean basins (Adcock et al., 2013).

This model of turbine characteristics is not strictly valid at the seaward end of the fence where flow can bypass the turbine array creating a much more complex flow and mixing regime locally. In this study we assume that any errors introduced by end effects will be negligible compared to the total power of the array, although this may be questionable for shorter arrays and hence we avoid analysing tidal turbine fences with lengths less than 500 m. A detailed analysis of the different mixing scales is described in Nishino & Willden (2012).

In this paper we use the convention of describing the length of a row as extending to half way across the edge beyond the last node defined as containing turbine. Computationally, as described above, this edge will contain a turbine with a blockage half that of the rest of the array.

2.3 Idealised domain

In this study we consider a headland in a wide channel as shown in Figure 1. The boundary A is forced

with a tide with amplitude 2 m and period 12.42 hours. The water level on boundary C is held constant. The tidal amplitude at these boundaries is not altered when changes are made within the domain and thus could represent the boundary between a continental shelf and a very deep ocean. Boundaries B and C are land boundaries. The headland extends 20 km into the channel. The simulation is run on a cartesian grid. Unlike the study of Draper et al. (2013a) the headland we study has a constant water depth around the area of the headland of 15 m. Whilst most physical headland sites do get deeper further from the shore the slope is often rather shallow and so general results derived from a site with a flat bed are likely to be qualitatively applicable to most real sites.

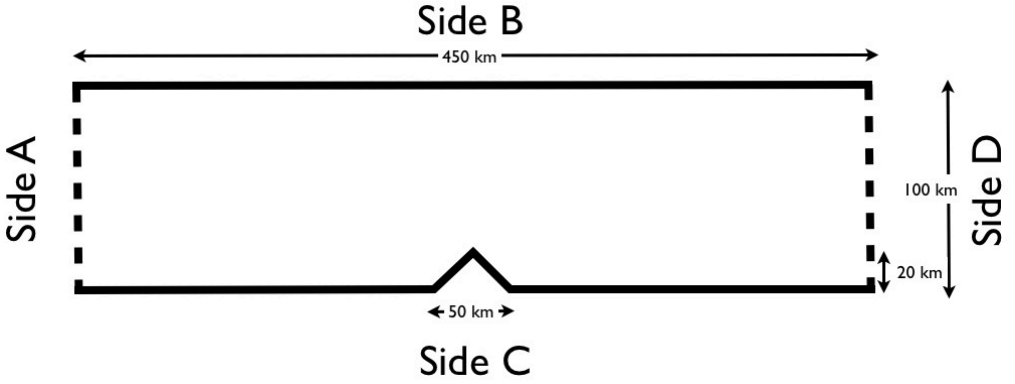

Figure 1 Schematic of the domain used in this study. Land boundaries are shown with thick solid lines. Ocean boundaries are shown with thick dashed lines.

The domain is meshed as shown in Figures 2 and 3. The mesh is mainly unstructured except for two rows at the end of the headland where turbines are placed. The model uses a bed friction coefficient of 0.0025 which is in the range typically applied to tidal models.

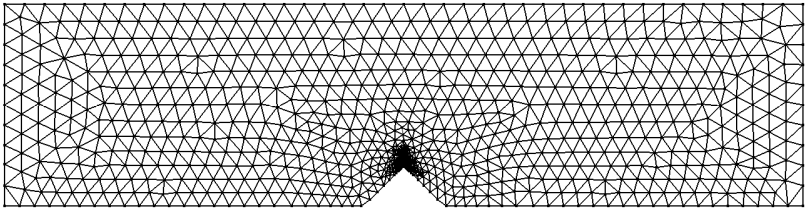

Figure 2. Numerical mesh used in study.

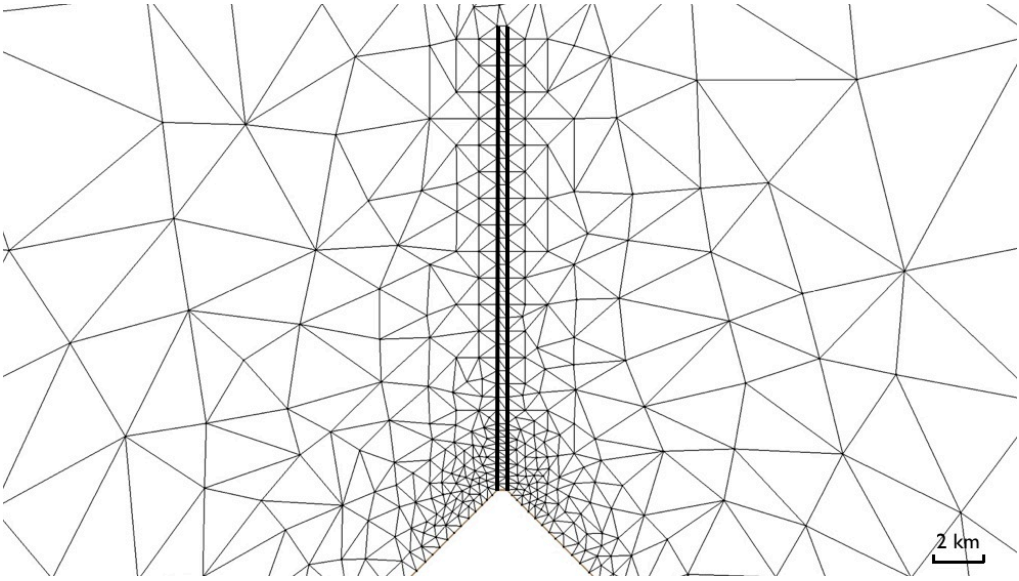

Figure 3. Close up of numerical mesh around headland. Turbines are shown with thick black lines.

3. Undisturbed flow characteristics

The model was allowed to 'spin up' for one day before starting the analysis. The model produces a fast flowing current around the tip of the headland, and separation occurs behind the headland. The flow is not symmetric – there is a stronger current moving left-to-right than right-to-left. Figure 4 shows the magnitude of the M_2 tidal component.

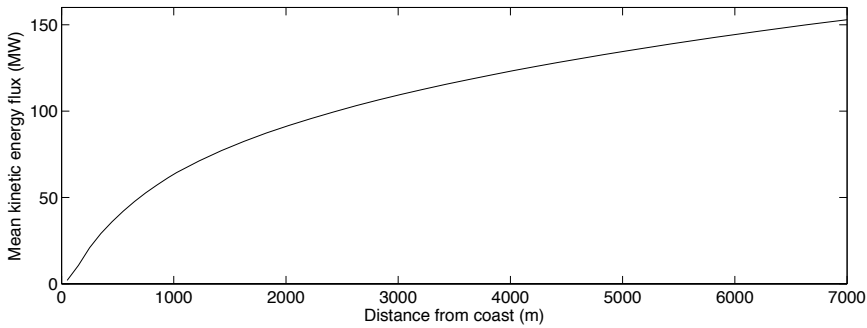

Figure 4 M_2 current magnitude (m/s) in the absence of tidal turbine. Turbine locations shown with white lines.

Draper et al. (2013a) has demonstrated that the natural kinetic energy flux does not determine the total resource of a site and is neither an upper, nor a lower bound to this. Despite this, kinetic energy flux is a useful metric for understanding a site and has been widely used in the past. Figure 5 shows the sum of the kinetic energy passing between the tip of the headland and a point directly offshore of it. The kinetic energy flux is strongest closest to the headland and reduces further offshore. For example, the kinetic energy flux between a point 1200 m from the headland and the tip of the headland is approximately the same as between 1200 m from the headland and 7000 m.

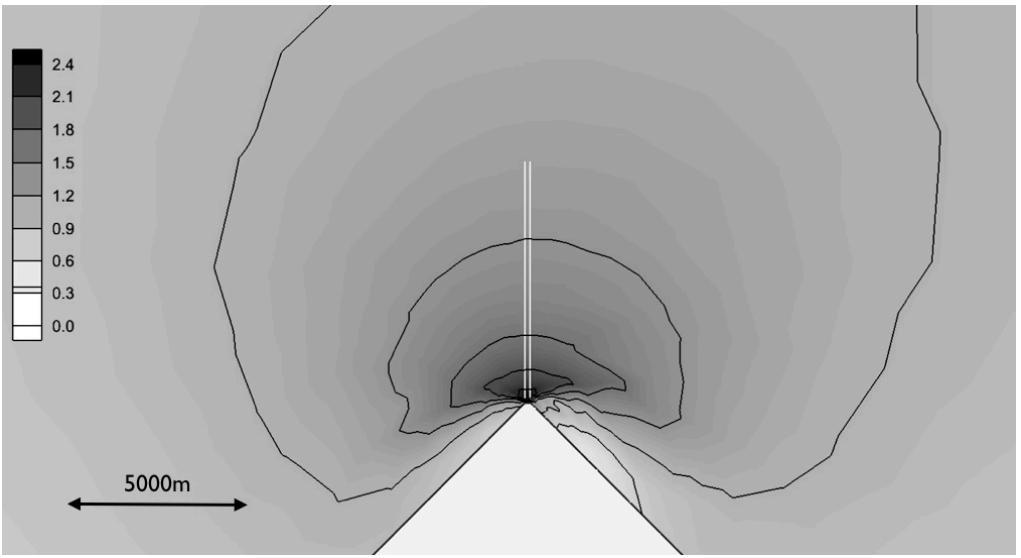

Figure 5. Sum of the kinetic energy flux passing between the headland and a point located a distance offshore from the headland.

4. Optimal distribution of turbine parameters

If the current is unaffected by the tidal turbines then the best performing turbine, in terms of available power, will have a wake velocity coefficient, $\alpha_4 = 0.33$ (for α_4 notation see Houlsby et al.2008). In real tidal flows there will be a reduction in the flow due to the presence of the turbine and in this case a larger α_4 (implying a smaller drag and therefore less reduction in current) may give a greater available power (Vennell, 2010).

To find the turbine characteristics that maximise the available energy we have to run a series of simulations with different turbine properties and analyse these to find the optimum. However, the value of α_4 which maximises energy extraction will vary across the width of a turbine fence as different parts of the fence experience currents of differing magnitude.

In this paper we approximate the optimum distribution of α_4 along a turbine fence as being linear and define this using the values at each end of the array. The true optimal layout is unknown. We have considered more complicated functions which do yield small increases in available power (a few percent) and of course the true optimum will be still higher. However, to search for this optimum for all cases would require an unfeasible computational effort. However all the results presented in this paper

will underestimate the true maximum available power but this effect is too small to effect the conclusions drawn from this work.

Figure 6 shows how the dependence of available power on the wake velocity coefficient for a range of turbine lengths where the blockage ratio is 0.5. These show that even for this very high blockage, the peak available power is relatively insensitive to the exact values of α_4. We can also see that the benefit of varying the wake velocity coefficient across the length of the turbine is typically relatively small (~ 5%). Such a small improvement in available power implies that a reasonable estimate of the available power for a site might be obtained without considering the variation in turbine properties across the site. However, in real sites the flow profile will be more complex than the one we are considering here so it is clearly desirable that a study such as this should be undertaken in the analysis of real locations.

This study indicates that it is preferable to have turbines operating with a lower wake velocity coefficient at the seaward end of a turbine row than at the land end.

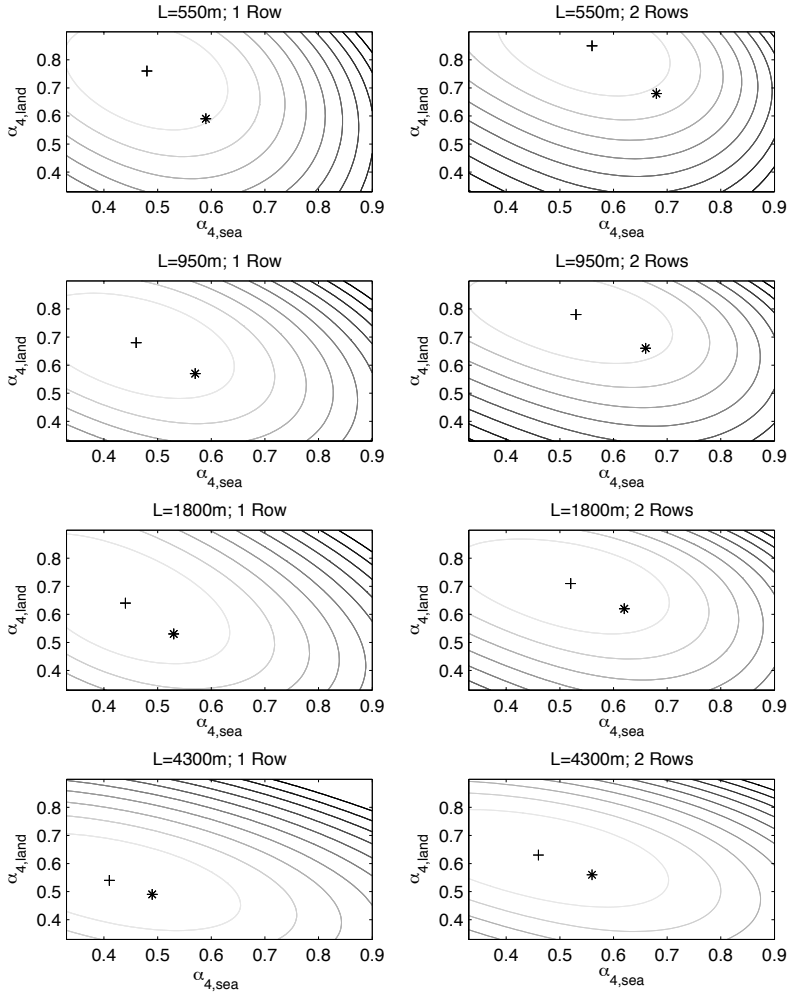

Figure 6 Available power for different wake velocity coefficients. Contours are available power normalised by maximum available power and are in gaps of 0.05 between 0.5 and 1 with 0.5 the darkest. The optimum location for a linear variation in α_4 is shown with a plus; the optimum location for a constant α_4 is shown with an asterisk.

We note that it might that a further improvement in the turbine performance may perhaps be achieved by varying the temporal properties of the turbines either over a short timescale (Adcock, 2012; Vennell & Adcock, 2014b) or over the longer spring/neap cycle (Adcock & Draper, 2014). These are not considered further here.

5. Results

In this section we investigate how the available power varies with the length and number of turbine fences. Two blockage ratios are considered: a 'high' blockage ratio of 0.5 and a 'small' blockage ratio of 0.1. The object of this is to show the different trends for two extremes of blockages.

Figure 7 shows how the available power varies with length of turbine fence. In all cases the available power increases as turbine rows are made longer and as additional rows are deployed. These curves may be compared to the naturally occurring kinetic energy flux (Figure 5). In all cases considered here the available power is less than the naturally occurring kinetic energy flux. For low blockage cases there is little change to the flow and the available power is primarily determined from the kinetic energy flux and the graph of available power is close in shape to that of kinetic energy flux. However, for higher blockages the curve is rather flatter — for instance, for two rows of high blockage turbines of length ~1200 m will have an available power of less than a third of two rows of turbines ~7000 m, whereas a prediction based on naturally occurring kinetic energy flux would be that the ~1200 m turbines would have half the power of turbines extending ~7000 m.

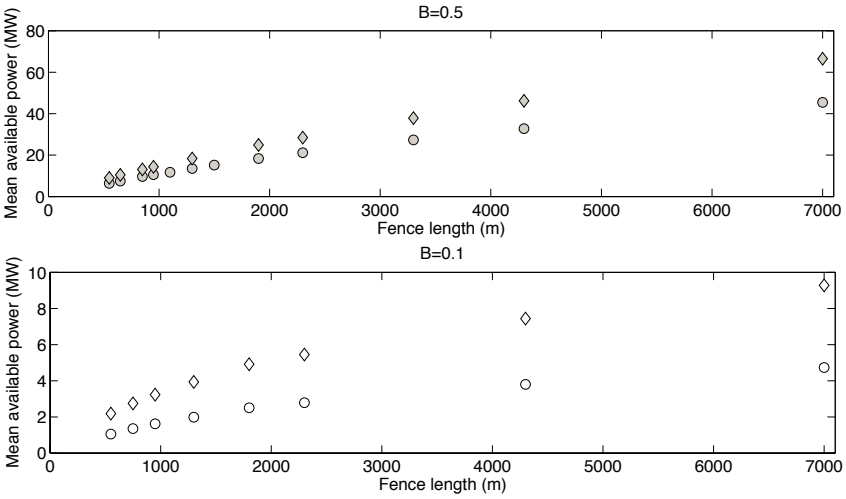

Figure 7. Available power for different lengths of turbine fence and different blockage ratios. Circles denote one row of turbines; diamonds denotes two rows.

Figure 8 shows how the power per swept area varies for one and two rows of turbines. For each specified number of rows and blockage ratio there is a decrease in the power per area as the total area increases. This is expected as the increased area is extending the turbine rows further offshore into areas where the naturally occurring current is weaker. There is a slightly different trend for short rows of highly blocked turbines. This is possibly due to the longer rows preventing flow from diverting around the turbines. It is plausible that in a different geometry there might even be a peak in this curve .

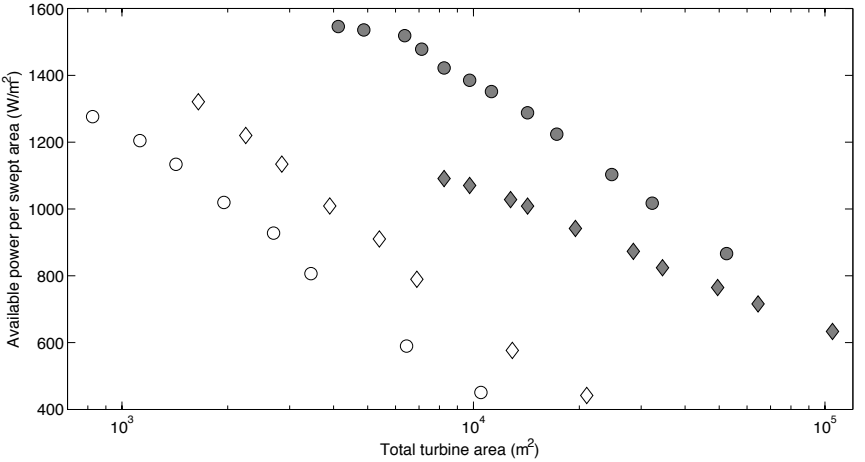

Figure 8 The available power per swept area against the total area of turbines deployed. Grey symbols show B = 0.5 and white symbols B = 0.1. Circles indicate one row of turbines and diamonds two rows.

There is a significant difference between the trends for high local blockage and low local blockage as additional rows are added. For highly blocked turbines, for a given total area of turbine and local blockage, it is always advantageous to arrange them as a single line rather than in rows close to the headland. Conversely, for the low blockage case, for a given total swept area, the maximum available power is achieved by deploying two rows of half the length.

This can be explored further by studying additional rows of low blockage turbines. Rather than include additional rows directly in the model we use the approximate method described in Draper et al. (2013a). This method is based on using an equivalent head loss, over two rows in this case, to represent the headloss over multiple rows. The available power can then be found from the efficiency of the turbine given in Houlsby et al. (2008). Figure 9 explores the effect of adding multiple rows of low blockage turbines for three different row lengths. With the exception of moving from one to two rows (presumably due to local effects) there is a steady decrease in the power per area as a greater total area of turbines are deployed. For a given total turbine area, the configuration which gives the optimum available power changes as greater area is added. When only a small swept area of turbines are considered it is preferable to exploit the strongest currents close to the headland. Adding greater number of rows, allows the turbines to apply a greater thrust to the flow and to be operated more efficiently. However, there is a diminishing return of available power as additional rows are added and so there is a limit where instead of adding extra rows, it is preferable to increase the length of the rows. For the example considered in this paper this limit appears to be around two rows for the low blockage case, and a single row when high blockage is used.

Extracting energy from a tidal current requires a thrust to be applied to the flow. This causes a change in the flow around the headland. Figure 10 examines the change in the M_2 tidal component for different lengths of turbine row, at peak available energy extraction for one row of highly blocked turbines. At peak available power there is a considerable reduction in the flow through the area where turbines are deployed. There is also an increase in the flow passing offshore of the turbines. The presence of turbines

is evidently causing the flow to be diverted around the end of the turbines. This diversion cannot occur in the idealised channels considered by (Garrett & Cummins, 2005; Vennell, 2010). The magnitude of the diversion is obviously related to the thrust the turbines exert on the flow. Thus, the metric of basin efficiency (the ratio of useful energy to energy extracted from the flow) will be relatively more important for turbines placed at headland sites than turbines placed in channels.

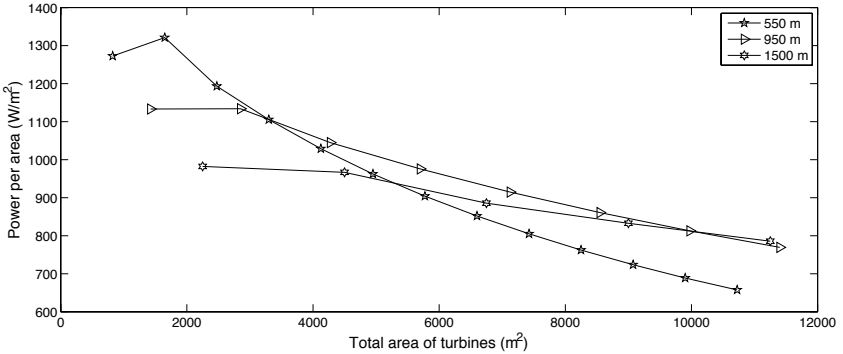

Figure 9 The power per swept area for different numbers of rows of turbines with blockage 0.1. For turbine rows of 550 m results from thirteen rows are shown; for turbine rows 950 m results from eight rows are shown; for turbine rows 1500 m results from five rows are shown.

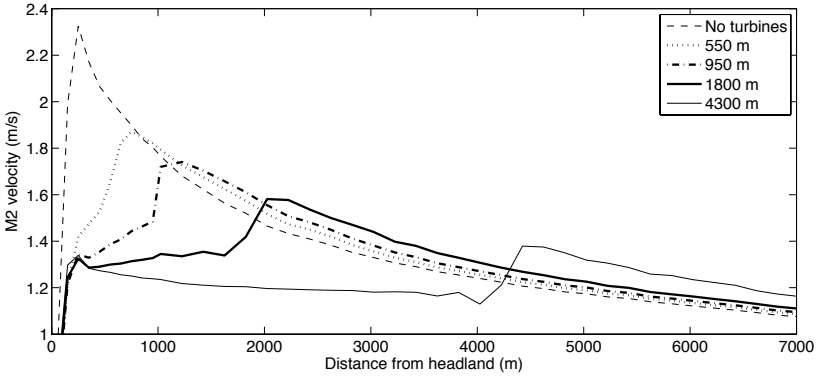

Figure 10. Magnitude of M_2 tidal current component at peak available energy extraction. For one row of turbines with B=0.5.

6. Conclusions

This study has analysed an idealised headland in a channel with the aim of drawing some general conclusions regarding the resource assessment and design of tidal farms at headland sites. A depth-intergrated numerical model of a headland has been set-up and actuator disc theory used to model the effect of tidal turbines within the model. A high and a low blockage ratio are considered.

We find that it is always hydrodynamically favourable to use the higher blockage ratio as this can extract energy with lower mixing losses than low blockage turbines. As more rows of turbines are

added there is a diminishing return and in general it is advantageous to extend one or two rows of turbines further from the headland than to install multiple rows close to the headland.

References

Adcock, T. A. A. 2012 On the Garrett and Cummins limit. *Oxford Tidal Energy Workshop, 29 – 30 March, Oxford, UK*.

Adcock, T. A. A., Draper, S., Houlsby, G. T., Borthwick, A. G. L. & Serhadlıoğlu, S. 2013 The available power from tidal stream turbines in the *Pentland* Firth. *Proceedings of the Royal Society A* 469 (2157), 20130072.

Adcock, T. A. A. & Draper, S. 2014a On the tidal stream resource of two headland sites in the English Channel: Portland Bill and Isle of Wight. *Proceedings of the 33rd International Conference on Ocean Offshore and Arctic Engineering, San Francisco, USA*. OMAE2014-23032.

Adcock, T. A. A. & Draper, S. 2014b Power extraction from tidal channels – multiple tidal constituents, compound tides and overtides. *Renewable Energy* 63 797 – 806.

Blunden, L. S. & Bahaj, A. S. 2006 Initial evaluation of tidal stream energy re- sources at Portand Bill, UK. *Renewable Energy* 31, 121–132.

Draper, S., Houlsby, G. T. & Borthwick, A. G. L. 2013a Energy potential of a tidal fence deployed near a coastal headland. *Phil. Trans. R. Soc.* A 371 (1985).

Draper, S, Houlsby, G T, Oldfield, M. L. G. & Borthwick, A. G. L 2010 Modelling Tidal Energy Extraction in a Depth-Averaged Coastal Domain. *IET Renewable Power Generation* 4 (6), 545 – 554.

Draper, S., Stallard, T., Stansby, P., Way, S. & Adcock, T. 2013b Laboratory scale experiments and preliminary modelling to investigate basin scale tidal stream energy extraction. In 10th European Wave and Tidal Energy Conference (EWTEC), Aalborg, Denmark.

Garrett, C. & Cummins, P. 2005 The power potential of tidal currents in channels. *Proceedings of the Royal Society A* 461 (2060), 2563–2572.

Houlsby, G T, Draper, S & Oldfield, M 2008 Application of Linear Momentum Actuator Disc Theory to Open Channel Flow. Technical report 2296-08. University of Oxford.

Kubatko, E. J., Bunya, S., Dawson, C., Westerink, J. J. & Mirabito, C. 2009 A performance comparison of continuous and discontinuous finite element shallow water models. *J. Sci. Comput*. 40 (1-3), 315–339.

Kubatko, E. J., Westerink, J. J. & Dawson, C. 2006 hp Discontinuous Galerkin methods for advection dominated problems in shallow water flow. *Computer Methods in Applied Mechanics and Engineering* 196 (1-3), 437 – 451.

Nishino, T. & Willden, R.H.J. 2012 The efficiency of an array of tidal turbines partially blocking a wide channel. *J. Fluid Mech*. 708, 596 – 606.

Serhadlıoğlu, S., Adcock, T.A.A., Houlsby, G.T., Draper, S. and Borthwick, A.G.L. 2013a Tidal Stream Energy Resource Assessment of the Anglesey Skerries, *International Journal of Marine Energy* 3-4 e98-e111.

Serhadlıoğlu, S., Houlsby, G. T., Adcock, T. A. A., Draper, S. & Borthwick, A. G. L. 2013b Assessment of Tidal Stream Energy Resources in the UK Using a Discontinuous Galerkin Finite Element Scheme. In FEF February 24-27 2013, San Diego, California.

Stansby, P. K. 2006 Limitations of Depth-averaged Modeling for Shallow Wakes. *Journal of Hydraulic Engineering* 132 (7), 737 – 740.

Vennell, R. 2010 Tuning turbines in a tidal channel. *J. Fluid Mech*. 663, 253–267.

Vennell, R. & Adcock, T. A. A. 2014 Energy Storage Inherent in Large Tidal Turbine Farms. *Proceedings of the Royal Society A*, 20130580.